Extended summary of the dissertation:

# "Label-free bioanalysis based on Whispering Gallery Modes: Development and practical application of low-Q microsensors"

Mateusz Olszyna

## 1. Introduction

In the last decade, a growing number of studies devote to the development of label-free analytical methods, contribute to faster and more reliable diagnosis of many human diseases such as cancers,[1,2] autoimmune diseases[3] or pathogenic infections.[4,5] In compare to common analytical techniques require labeling target molecules with fluorescent or radioactive markers to make the specific binding events visible, label-free methods exploit optical,[6,7] electrical[8] or mechanical[9,10] transducer mechanisms to translate the binding information into a measured signal. This approach allows eliminating time- and cost-consuming molecules modification keeps their structure, surface charge and bioactivity intact. In particular, the label-free biosensing systems applying optical transducer mechanism such as surface plasmon resonance (SPR),[11] biolayer interferometry (BLI)[12] or reflectometric interference spectroscopy (RIfS)[13] are rapidly gaining in popularity because of their fast assay development time, real-time kinetic analysis, possibility of automation and high sensitivity. However, the high sensitivity is achieved usually by applying planar and relative large (in the range of millimeters) transducer. This significantly limits the use them in small volumes such as cell arrays or even inside cells. Furthermore, the large geometry often requires temperature stabilization which in turn leads to high instrumental efforts and price. Based on these limitations, micrometer-size spherical sensors such fluorescent Whispering Gallery Modes microresonators proposed in this work, seems to be a promising concept in new-generation label-free diagnostic systems.

### 1.1 Whispering Gallery Mode (WGM)

Whispering Gallery Modes (WGMs) are specific eigenmodes of natural waves (e.g. acoustic waves, electromagnetic waves or various subatomic particle waves) circulating around a concave surface (a cavity). This circulation is supported by continuous total internal reflection (TIR) at an interface of cavity and medium and allows building constructive interference (**Figure 1a**). WGM resonance can only be formed when the length of the optical path equals an integer number of wavelengths inside the resonator and depends greatly on its radius as well as

refraction index. Traditionally, the term whispering gallery mode refers to electromagnetic surface oscillation occurring in dielectric cavities.[14]

a) b)

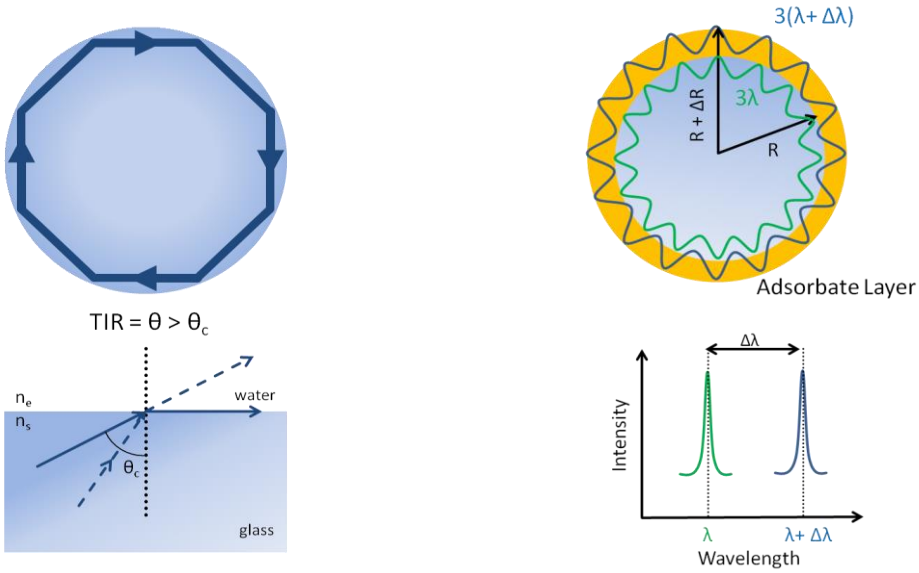


**Figure 1**. Total internal reflection (TIR) in spherical resonator (a) and schematic illustrating the change in path length taken by light upon the adsorption of material to the surface of spherical WGM microresonator (b).

The fundamental sensing principle of WGMs resonators is based on measuring changes in resonance frequencies as result of chemical-physical modifications on the surface. As the light is reflected at the cavity edge, a portion of photons extends around 100-200 nm outside the cavity forming the so called evanescent wave.[15] This wave propagates tangent to the surface and is characterized by its high sensitivity to any changes in optical geometry or refractive indices of resonator as well as the surrounding environment. Binding of nanoparticles or single molecules on the resonator' surface increases the optical path length of the photon orbit, perturbing at the same time the resonance profile[15] (**Figure 1b**). This change is detectable as a shift (Δλ) in the spectral position of a WGM resonance and can be calculated according to the fundamental equation:[15,16]

$$\Delta\lambda = \frac{2\pi n_s \Delta R}{l} = \lambda \frac{\Delta R}{R} \qquad (1)$$

Here, λ is wavelength of the WGM with the integer mode number $l$, $n_s$ the refractive index of the sphere, R its radius and ΔR increase of sphere radius by adsorbate layer.

Depending on the polarization of light, two types of WGMs can be distinguished: transversal magnetic modes (TM-modes) and transversal electric modes (TE-modes). In the TM-mode, the

magnetic fields are perpendicular to the normal of the sphere surface and parallel to the direction of light propagation, whereas in the TE-mode the electric fields are parallel to the normal of the sphere surface and perpendicular to the direction of light propagation[17] (**Figure 2**). From a practical point of view, the wavelength shift of TM-modes is usually bigger than for TE-modes because of perpendicular orientation of the adsorbed molecules to resonator's surface.

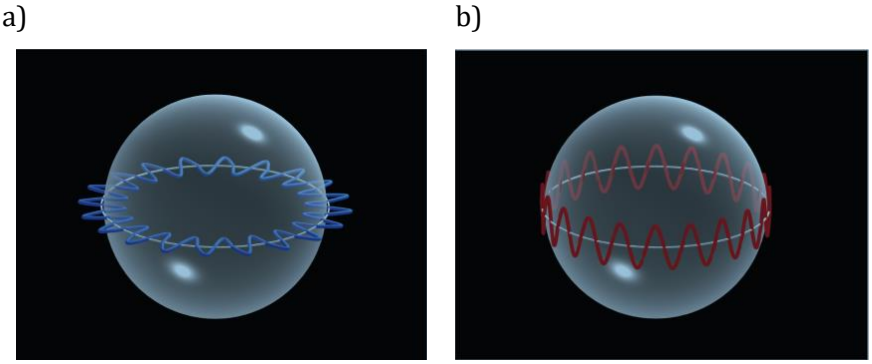


**Figure 2.** Schematic illustrating of two polarization modes in spherical resonator: transversal magnetic modes (TM-modes) (a) and transversal electric modes (TE-modes) (b). Adapted from [18].

Typically, the WGM sensor performance is characterized by two parameters: quality factor (Q-factor) and the magnitude of wavelength shift. Q-factor described the rate of energy loss of light during circulation within the cavity and can be mathematically expressed as a ratio of the mode's wavelength and full bandwidth at half-maximum ($Q = \lambda_m / FWHM$).[14,15,19,20] Based on Q-factor, two types of WGM resonators can be distinguished. First type, the high-Q WGM resonators are able to confine light over a long time period (from $10^4$ up to $10^6$ recirculations)[21] because of their large diameter (typically d = 100-200 μm)[15,22] and therefore minimal intrinsic reflection losses. Due to smaller curvature and better TIR conditions, high-Q WGM resonators exhibit extremely narrower mode bandwidths (0.01 - 2 pm) and thus higher sensitivity of detection.[15,21,22] However, their sensing performance is partially diminishing by smaller relative mode shift and spectral density (distance between following modes) carrying precise information about resonator diameter. The second type, low-Q WGM resonators, present significantly broader bandwidths (typically in the range of 0.02-0.2 nm) but higher relative mode shift.[16,23] Furthermore, due to small diameter (d < 12 μm), they require much less analyte molecules[25] and offer possibility of incorporation in cavities down to cell size or even below.[23,24] The use of polymeric materials to produce low-Q WGM sensors such as polystyrene or melamine formaldehyde allows to incorporation of fluorescence dyes[16,23-25] or quantum dots[26] inside of the particles and remote WGMs excitation by an external light source, i.e. diode laser (**Figure 3a**). In compare to high-Q WGM systems, this approach eliminates the need for awkward evanescent

field coupling making the low-Q WGM sensors easier in handling, remotely operable and opens an opportunity for multiplexing and comercialization.[24-25]

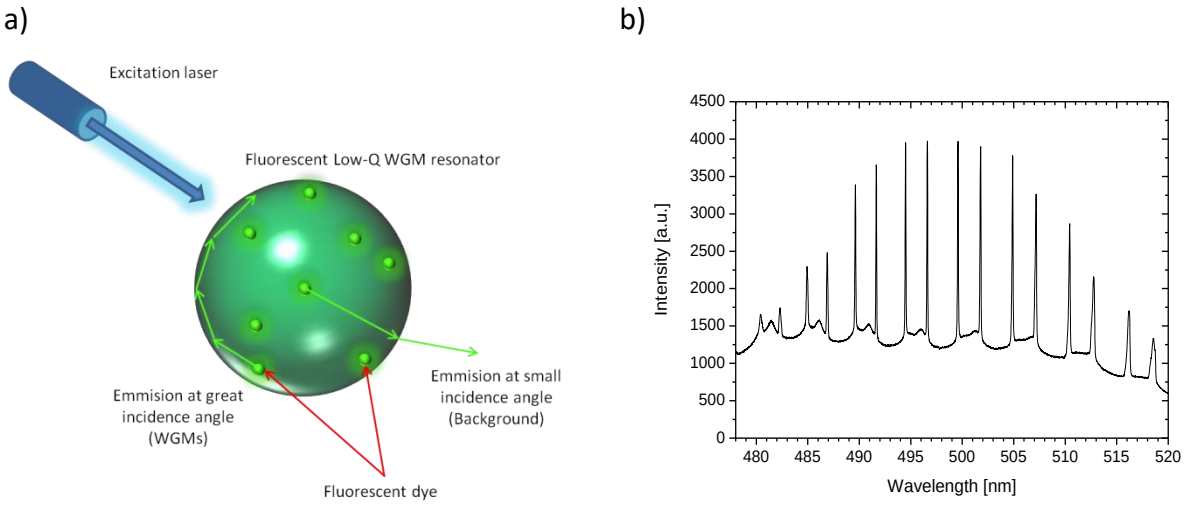


**Figure 3.** Principle of fluorescent low-Q WGM resonators (a) and typical WGM spectra of fluorescent polystyrene microbeads (b) (nominal diameter 11µm, measured in water).

## 2 Aim of this work

Based on current challenges in development of label-free biosensors systems applying WGM excitation in fluorescent polymer microbeads as the optical transducer mechanism, this thesis had the following aims:

(i) Development and optimization of fluorescent low-Q WGM microsensors

(ii) Practical application of fluorescent low-Q WGM microsensors in label-free bioanalysis

Aim (i) was pursued in the frame of studying the influence of resonator's type and size, polymerization method, fluorescent dye and dye distribution for the quality and stability of WGM signal.

For aim (ii) the unspecific binding of polyelectrolytes and protein on WGM microsensors were tested. In order to demonstrate the performance and practical usability of the developed WGM microsensors, specific interactions of biotinylated molecules on streptavidin-modified sensor surface were studied.

## 3 The main results of the dissertation

The results of the thesis were divided into two parts. First part dealt studies of the effect of microparticle material type, refractive index, surface roughness as well as the particle polymerization method and size on WGM performance. Besides of this, a comparison of selected fluorescent dyes and dye distribution methods in case of stability and intensity of WGM signal

was invesitgated. The second part demonstrated the practical using of the low-Q WGM sensors in label-free bio-analysis. In this case, the unspecific adsorption of polyelectrolytes and proteins based on ion attraction and hydrogen bonding as well as specific interactions of biotinylated molecules on streptavidin-modified sensor surface was investigated.

## 3.1 Development and characterization of fluorescent low-Q WGM microsensors

As known from fundamentals, many physical properties of resonators such as morphology (including shape, size and surface roughness), density, refractive index or even mechanical strength, affecting their TIR conditions and as consequence the WGM performances. Therefore, the right choice of these parameters is the crucial point in produce low-Q WGM microsensors.
This summary presents the results of three key aspects in fabrication low-Q WGM microsensors: selection a suitable resonator material type, choice of polymerization method and determination an optimal dye distribution method.

### 3.1.1 Screening of low-Q WGM microparticle material type

The study of the effect of microresonator material type, refractive index and surface roughness on WGM performance was carried out for four spherical microparticle types: polystyrene (PS), melamine formaldehyde (MF), polymethylmethacrylate (PMMA) and borosilicate glass (BG) with RIs of 1.59, 1.68, 1.48 and 1.55, respectively and nominal diameter of 8-10 µm. All particle types were fluorescently labeled by using of Layer-by-Layer coating technique. The microparticles were characterized by using of WhisperSense instrument, scanning electron microscopy (SEM) and atomic force microscopy (AFM). The real RIs were determined using Airy approximations and formula proposed by Pang et al.:[26]

$$\lambda_{TM}\ (q = 1)\ = 2\ n_s \pi R \left[ v + 1.8557 v^{1/3} - \frac{n}{\sqrt{n_c^2 - 1}} + 1.0331 v^{-1/3} - \frac{1.8557(n_c^4 - \frac{2}{3})}{n_c^3 (n_c^2 - 1)^{3/2}} v^{-2/3} + O(v^{-1}) \right]^{-1} \quad (2a)$$

$$n_c = \frac{n_s}{n_e}, v = l + \frac{1}{2} \quad (2b)$$

Here, $\lambda_{TM}$ is wavelength positions of first order (q = 1). The value $v$ is the order of Bessel function involved and related to mode number $l$. $n_c$ is the contrast RI at the resonator ($n_s$)/environment ($n_e$) interface and R is the particle radius.

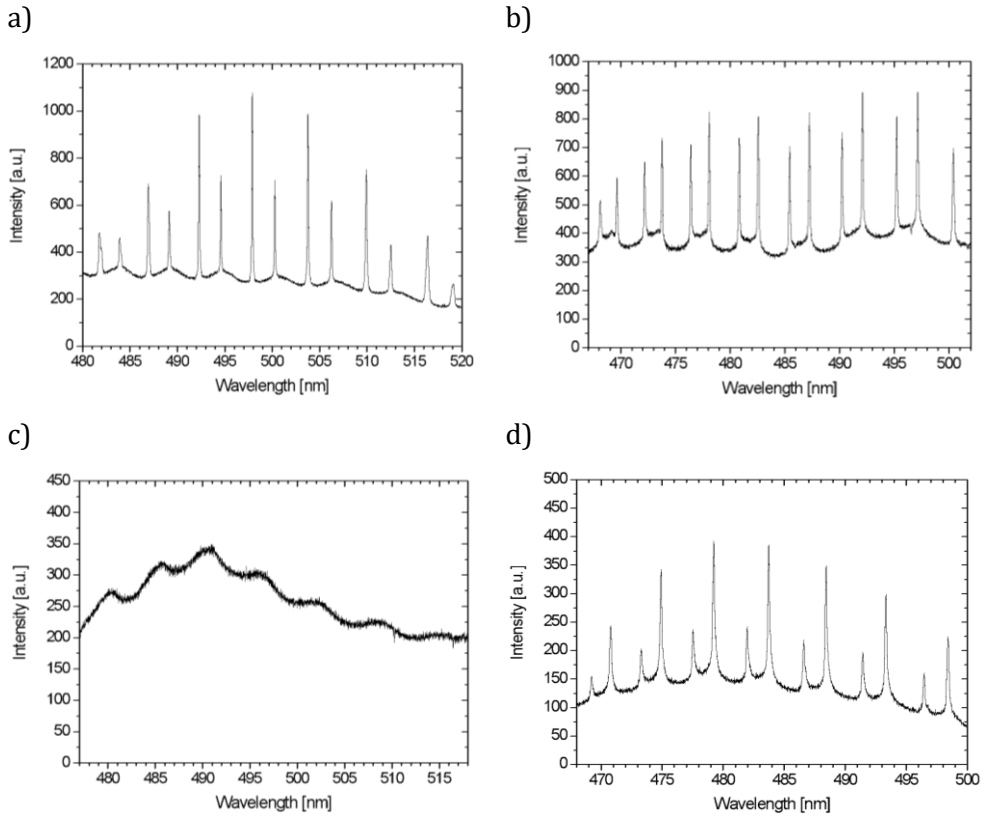


**Figure 4.** WGM spectra of different microparticle materials fluorescently labeled using LbL technology (a) Polystyrene (PS) beads; diameter 9.3 μm. (b) Melamine formaldehyde (MF) beads; diameter 8.8 μm. (c) Poly (methyl methacrylate) (PMMA) beads; diameter 10.7 μm. (d) Borosilicate glass (BS) beads; diameter 10 μm.

The results show that PS particles yield the highest intensity and narrower bandwidth of WGM (**Figure 4a**). MF and BG particles exhibit slightly broader WGMs than PS particles but significantly higher background noise and more side peaks (**Figure 4b, d**). PMMA particles gave almost no WGM signal (**Figure 4c**). Measurements performed by SEM and AFM reveal that only PS particles have a homogenous and smooth surface. BG and PMMA beads show inhomogeneous surface with many clumps of synthesis resting. MF beads in turn exhibit small pores, which can be related to aggregation of nanoclusters during polycondensation of melamine and formaldehyde. On the basis of real RI values obtained by calculation the distance between subsequent TM-modes (**Table 1**), was found that MF particles exhibit significantly lower RI than that of bulk MF. The reason was related to differences in fabrication methods employed in producing bulk melamine resin and MF particles. Summarizing, it was found that PS particles are best suited sensors for WGM excitation, whereas MF, BG and PMMA due to their higher surface roughness and lower RIs show less quality.

**Table 1.** Refractive index of WGM beads

| Particle material | RI of bulk material (uncolored) | RI determined by WGM |
|---|---|---|
| Polystyrene (PS) | 1,59[a] | 1,55 |
| Melamine formaldehyde (MF) | 1,68[a] | 1,52 |
| Poly(methyl methacrylate) (PMMA) | 1,48[a] | data not available |
| Borosilicate glass (BG) | 1,55[b] | 1,52 |

Data obtained from: [a)] Microparticles GmbH; [b)] Polysciences Inc.

### 3.1.2 Selection of polymerization method

To find out an optimal polymerization method of styrene to produce low-Q WGM sensors, three polymerization variants were studied: dispersion, emulsion and seeded-growth polymerization. PS particles were examined in terms of their morphology, size distribution and WGM performances by using Confocal Laser Scanning Microscopy (CLSM), CPS disc centrifuge and WhisperSense instrument, respectively.

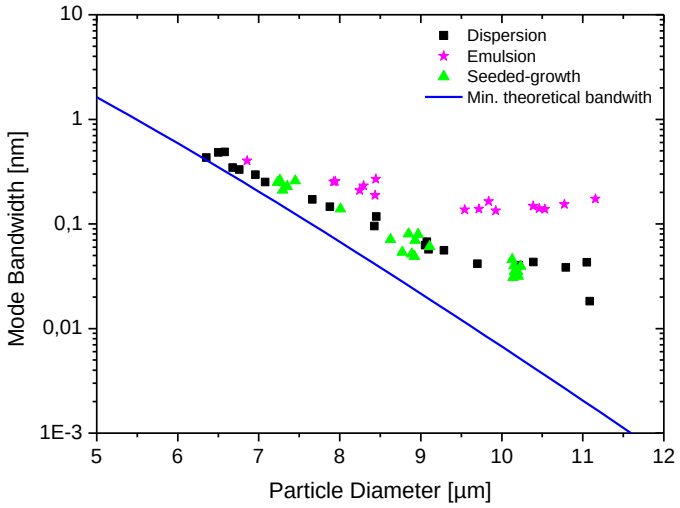


**Figure 5.** TM Mode bandwidth of PS particles synthesized by different polymerization methods. Blue line represents minimal bandwidth of ideal PS particles with RI = 1.58 (calculated according [16])

PS particles prepared by seeded-growth and dispersion polymerization show significantly narrower mode bandwidth than particles prepared by emulsion polymerization (**Figure 5**). However, in case of size distribution, was found that particles prepared by emulsion and dispersion polymerization exhibit strong polydispersity whereas particles prepared by seeded-growth polymerization show highly uniform size. The reason lies in the first steps in growing process of particles. For the first two types of polymerization i.e. dispersion and emulsion polymerization, the particles grow uneven because the polymerization starts regardless of

nanoparticle size and cannot be precise controlled. In contrast, particles fabricated via seeded-growth polymerization rise up simultaneously from seeds in the same size, therefore show finally high monodispersity. Summarizing, best suited polymerization method to fabrication polystyrene low-Q WGM sensors was seeded-growth polymerization because of high WGM performances, monodispersity and controllable particle size.

### 3.1.3 Determination the optimal dye distribution

In order to determine an optimal dye distribution in low-Q WGM microsensors, a three dyeing methods were investigated: standard dye-doping method, gradual solvent evaporation method[27] and fluorescent Layer-by-Layer coating technique (LbL).[25,28,29] Three types of fluorescently-labeled PS particles (nominal diameter of 10 μm) were analyzed in terms of their WGM performance, morphology and location of fluorophore molecules by using WhisperSense instrument and Confocal Laser Scanning Microscopy (CLSM). Additionally, in case of the LbL coating technique, the influence of layer number on WGM intensity and bandwidth was studied.

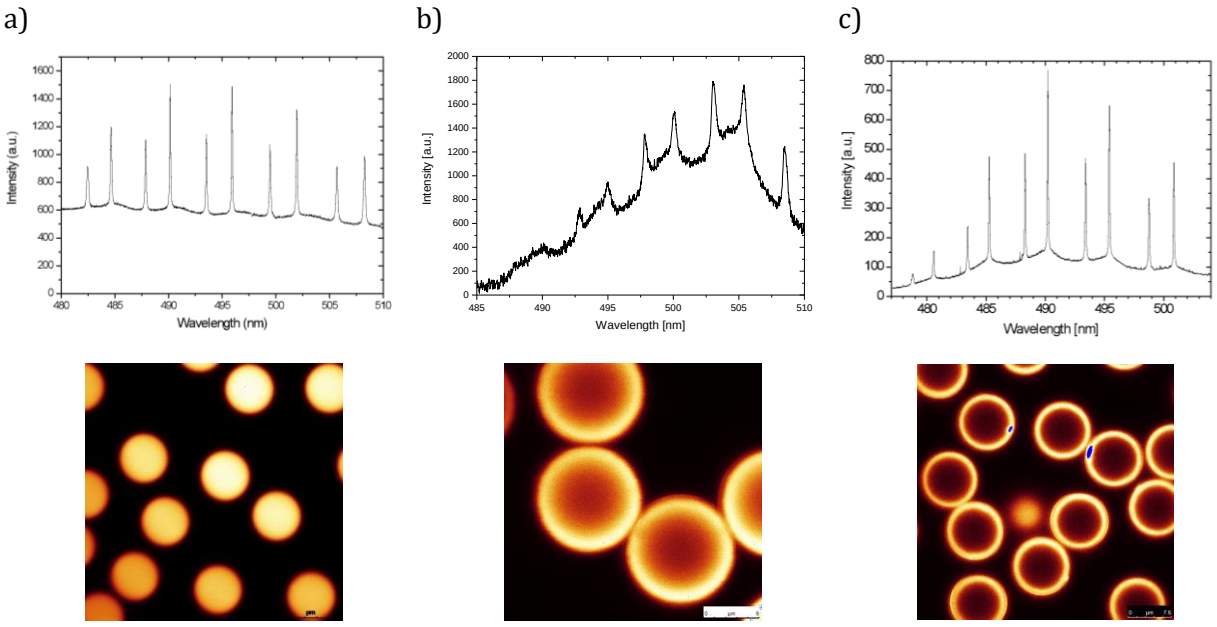


**Figure 6**. WGM spectra (top) and CLSM images (bottom) of PS particles labeled with different methods: dye-doped method (a), gradual evaporation method (b) and fluorescent LbL coating (c).

The best spectra, characterized by high intensity, narrow bandwidth and low background noise, were obtained for PS particles labeled by dye-doped and LbL method (**Figure 6a, c, top**). In contrast, particles dyed by gradual solvent evaporation method exhibit significantly broader and asymmetrical peaks with high background noise (**Figure 6b, top**). Furthermore, they show a high intensity between TM- and TE-mode, what can be an evidence the changes in particle shape or surface roughness during evaporation the dye solvent.

Taking into account the distribution of fluorescent dye, LbL technique allowed to immobilize dye molecules directly onto particle surface forming fluorescent, nano-scale thin film (**Figure 6c, bottom**). In compare to the standard dye-doped method, where fluorophore molecules are homogeneous distributed in the whole particle (**Figure 6a, bottom**), this approach offers several advantages such as higher peak/background ratio, easier (bio-) functionalization with a wide range of functional groups or more versatility of particle materials. However, the WGM signal intensity and bandwidth of particles coated LbL depends on the number of polyelectrolyte layers (**Figure 7**). With each polycation layer, the number of deposited dye molecules at the particle surface increases, which enhances the WGM signal intensity and bandwidth, whereas the background is only weakly enhanced. In contrast, homogeneously dye-doped particles exhibit comparable bandwidth but a strong background signal with slightly higher overall peak intensity. The high background signal of dye-doped particles arises from fluorophores far away from the surface, deeply embedded inside the particle. Their emitted light hits the interface always at angles above the angle of TIR and does not contribute to the WGM signal, while it is still observed by the spectrograph as background noise.

Summarizing, the immobilization of fluorescent dyes by LbL technique on non-fluorescent PS particles yields highly qualitative WGM sensors with narrow bandwidth, low background signal and easy post-modification possibility.

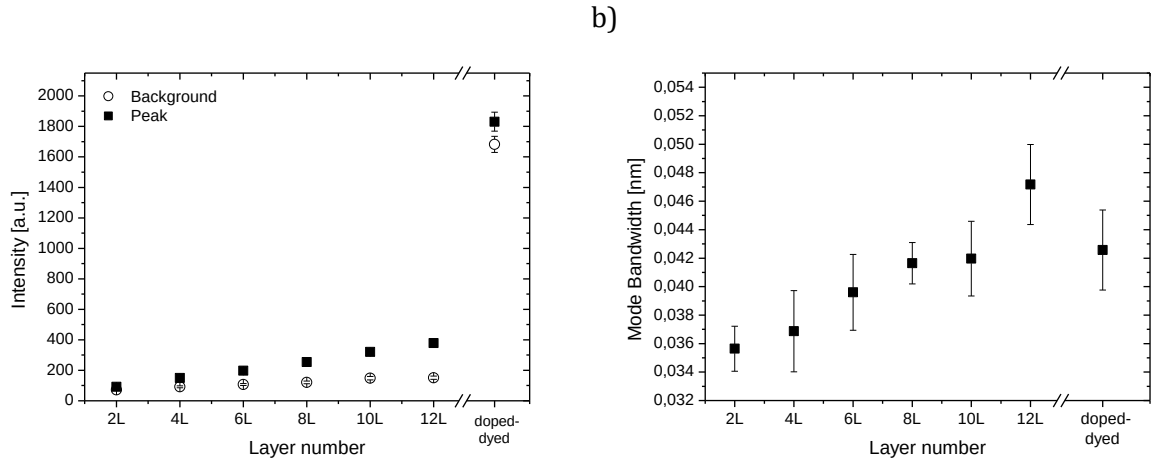


**Figure 7.** Characterization of doped-dyed and LbL fluorescently-labeled low-Q-WGM microresonators. Correlation between layer number and fluorescence intensity (a) and mode bandwidth of WGMs (b).

## 3.2 Label-free detection based on fluorescent low-Q WGM microsensors

In this part of thesis the practical applications of fluorescent low-Q WGM microparticles as novel label-free biosensors were demonstrated. This summary presents the results of two main analytical measurements: electrostatically adsorption of lysozyme onto opposite charge surface and specific interactions of protein based on streptavidin-biotin model.

### 3.2.1 Analyze of unspecific adsorption of lysozyme

In order to determine the real sensitivity of developed low-Q WGM microsensors, WhisperSense instrument was compared with well-established Biacore system by measurement the kinetic adsorption of lysozyme in different concentrations. In this case, optical transducers (spherical PS particles for WGM and planar goldchips for SPR) were LbL coated with positively charged polyelectrolyte (Polyallylamine (PAH)) and washed with negatively charged lysozyme (PBS buffer, pH 7.4) in different concentrations (1000, 100, 10, 5 and 1 µg/mL). In case of the WhisperSense instrument, obtained shift of TM-modes shift was converted to the adsorbed mass value by using formula proposed by Himmelhaus:[16]

$$\sigma = \rho \frac{\Delta V}{A} = \rho \frac{\frac{4}{3}\pi\left[(R + \Delta R^3) - R^3\right]}{4\pi R^2} = \frac{\rho}{3}\frac{(R - \Delta R)^3 - R^3}{R^2} \qquad (3)$$

Here, $\sigma$ is the surface mass density, $\rho$ is the mass density of adsorbate, R is the particle radius, $\Delta R$ is the change in particle radius, $\Delta V$ is the volume change and can be calculated from $\Delta R$ value and $A$ is the particle surface area.

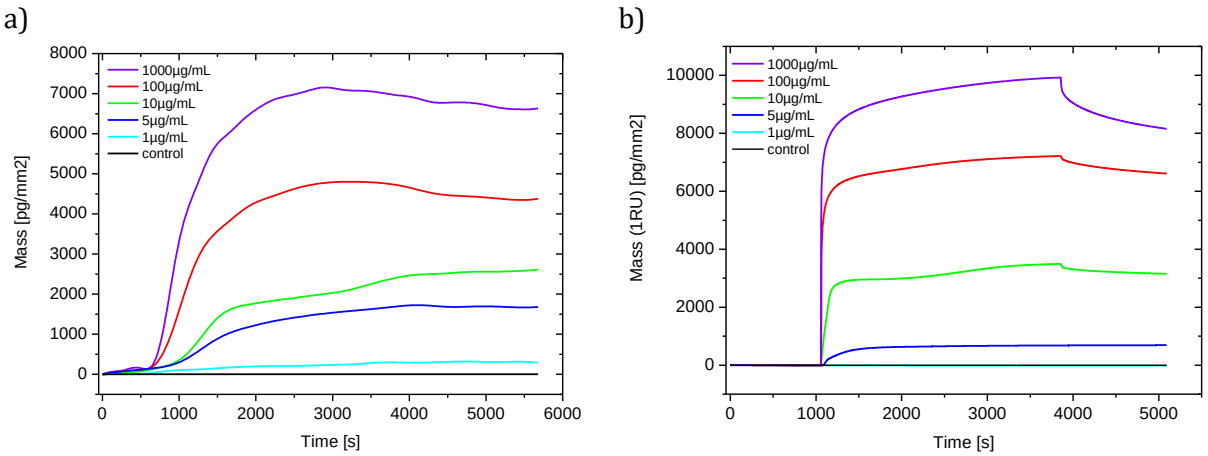


**Figure 8.** Adsorption kinetic of lysozyme in different concentration onto opposite charge polyelectrolyte measured in WhisperSense instrument (a) and Biacore system (b).

It was found, that the minimal detectable concentration of lysozyme is 1µg/mL measured in WhisperSense instrument and 5 µg/mL measured in Biacore system (**Figure 8**). However, the adsorption kinetics in Biacore instrument are significantly faster than in WhisperSense instrument and show a visible desorption of unbounded lysozyme. The reason can be related to the real flowrate and mass transport of protein in applying microfluidic systems. Biacore instrument uses a planar goldchip with very small microfluidic channels layout. It allows decreasing the flowrate (usually 40 µl/min) keeps the diffusion constants still in a high level. In contrast, WhisperSense instrument implements micropatterned microfluidic chips with

significantly bigger channel dimension.[24] It leads to slower diffusion of analyte and more flat kinetic adsorption curves.

Summarizing, WhisperSense instrument using low-Q WGM particle as microsensors can be successful applied in label-free biosensing and show comparable results of unspecific binding of lysozyme with other well-established label-free detection system such as SPR. However, due to slow adsorption kinetics of lysozyme and no discernible desorption the microfluidic channel have to be reconstruct.

### 3.2.2 Analyze the specific bio-molecular interactions based on streptavidin-biotin model

The ultimate test of overall system performance was accomplished by specific detection of a biomolecule. As a straightforward and widely used benchmark model for label-free performance testing, the biotin-streptavidin system was applied here. The first experiment deals the studies of determination the limit of detection of low-Q WGM sensors in different size (7 and 10µm) by measurement the amount of streptavidin binding on LbL-biotin-modified sensor's surface. The second experiment demonstrates a specifically functionalization of low-Q WGM sensor by coating the streptavidin-modified particle surface with biotinylated antibodies.

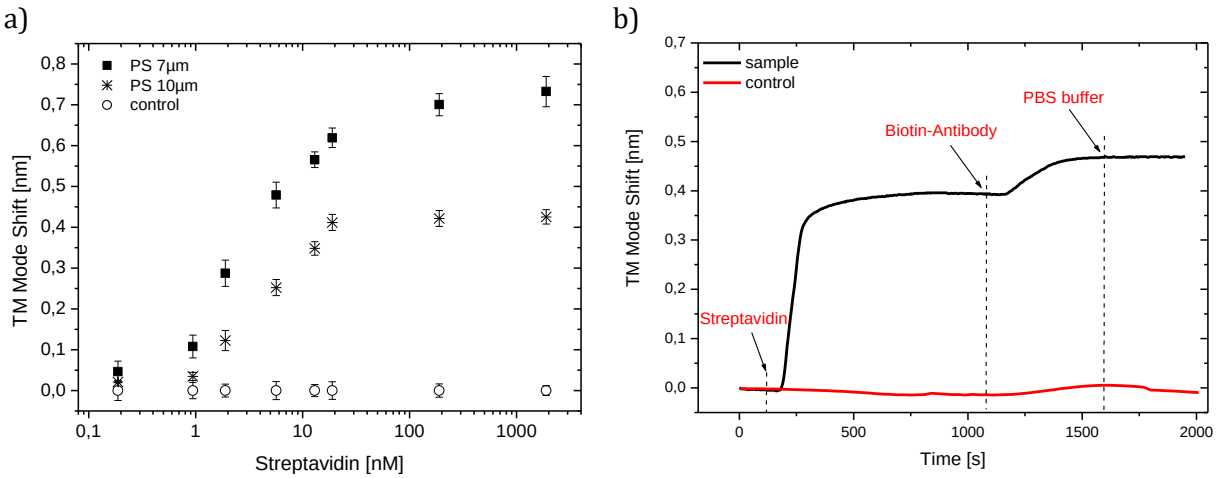


**Figure 9** Determination the limit of detection of low-Q WGM microsensors in 7 and 10µm diameter by adsorption of streptavidin onto biotinylated surface (a). Kinetic adsorption of biotinylated antibody onto streptavidin-modified low-Q WGM particle (b).

According to the fundamentals, WGM sensors with smaller diameter (7µm) show significantly bigger mode shift than large particle (10µm) (**Figure 9a**). However, as the streptavidin concentration decreases, the difference in mode shift for 7 µm and 10 µm particles also decreases. It can be related to the smaller number of adsorbed streptavidin molecules as consequence the deteriorated diffusion in lower concentrations. The limit of detection for streptavidin was determine to 0.2 nM for both particle size.

Streptavidin-biotin interaction were also used to specific modification the low-Q WGM sensors's surface with antibodies. PS particles coated first with biotinylated LbL film were then cover with streptavidin layer and finally with biotin-modified antibodies. The kinetic adsorption of streptavidin and biotin-antibody was measured in WhisperSense instrument. In order to exclude unspecific interactions, a control particles were coated with non-biotinylated LbL-film. The results show that biotinylated antibodies can be successfully attached onto streptavidin-biotin modified low-Q WGM particles. The pre-modification the sensor's surface with negatively charged LbL film allowed reducing the unspecific binding to a minimum.
Summarizing, developed low-Q WGM microsensors can be successfully used in label-free detection of specific biomolecules show very low limit of detection and easy functionalization.

# 4 Conclusions

The main objective of this work was to develop and characterize the low-Q WGM microsensors that can be successfully used in label-free detection of specific biomolecules. Hereafter more important conclusions are listed.

1. Best suited particle material type to produce low-Q WGM microsensors is polystyrene because of high signal intensity and narrow bandwidth. The studies using atomic force microscopy, scanning electron microscopy and whispering gallery modes biosensing confirmed their smooth surface and high refractive index.
2. WGM particles synthetized by seeded-growth polymerization showed high WGM performances, monodispersity and controllable particle size.
3. Optimal sensor size range was found between 8.5-11μm due to higher signal intensity, narrower bandwidth and easy data processing.
4. Coumarin 6 demonstrated best properties by means of WGM excitation in PS particles, including high resistance to photobleaching, short adsorption/emission wavelength, hydrophobicity and high values of molar extinction coefficient and quantum yield.
5. Immobilization of fluorescent dyes by LbL technique on non-fluorescent PS particles yields highly qualitative WGM sensors with narrow bandwidth, low background signal and easy post-modification possibility.
6. The studies of formation the LbL films performed in WGM sensing system showed the dependence between salt concentrations and layer thickness and confirmed the previous results from quartz crystal microbalance and ellipsometry.
7. The studies of unspecific adsorption of lysozyme in different concentrations performed in surface plasmone resonance and whispering gallery modes sensing system showed slightly better sensitivity of WGM but significantly slower kinetic adsorption than SPR.

8. The low-Q WGM microsensors were successfully functionalized by using of streptavidin-biotin interaction system. The limit of detection of streptavidin was measured by 0.2nM.

Based on the obtained results, it can be concluded that developed low-Q WGM microparticles are promising, new-generation biosensors to be used in label-free detection of many type of biomolecules such as proteins (including antibodies), DNA/RNA, viruses, bacteria or even drugs.

# 5 References


1. C. Kuepper et al. *Scientific Reports* **2018**, 8.
2. S. Lee, H. Chon, J. Lee, et al. *Biosens. Bioelectron.* **2014**, 51.
3. M. Miyara et al. *PLoS ONE* **2018,** 13(8).
4. C. Markwalter, I. Jang, R. Burton, G. Domingo, D. Wright, *Anal. Biochem.* **2017**, 534.
5. G. Anderson, J. Liu, D. Zabetakis, P. Legler, E. Goldman, *J. Immunol. Methods* **2017**, 442.
6. A. Washburn, M. Luchansky, A. Bowman, R. Bailey *Anal. Chem.* **2010**, 82.
7. R. Rich, D. Myszka, *Curr. Opin. Biotechnol.* **2000**, 11, 54–61.
8. Y. Bunimovich et al., *J. Am. Chem. Soc.* **2006**, 128, 16323–16331.
9. N. Backmann et al., *Proc. Natl Acad. Sci. USA* **2005**, 102, 14587–14952.
10. N. Kim, D-K Kim, Y-J Cho, *Sensor. Actuat. B-Chem.* **2009**, 143, 444–448.
11. J. N. Anker et al, *Nat. Mater.* **2008**, *7*, 442.
12. J. Conception et al., *Comb. Chem. High Throughput Screen* **2009**, 12, 791.
13. J. Piehler, A. Brecht, K. E. Geckeler, G. Gauglitz, *Biosen. and Bioelectro.* **1996**, 11, 579.
14. G. Righini et al., *Rivista del Nuovo Cimento* **2011**, 34, 435-488.
15. F. Vollmer, S. Arnold, *Nature Meth.* **2008**, 5(7).
16. M. Himmelhaus, S. Krishnamoorthy, A. François, *Sensors* **2010**, 10, 6257-6274.
17. M. Michihata, T. Hayashi, A. Adachi and Y. Takaya, *CIRP Annals* **2014**, 63(1), 469-472.
18. J. Topolancik, F. Vollmer, *Biophys. J.* **2007**, 92, 2223–2229.
19. A. Oraevsky, *Quantum Electronics* **2002**, 32, 377-400.
20. A. Bozzola, S. Perotto, and F. De Angelis, *Analyst, Royal Society of Chemistry* **2017**, 142, 883-898.
21. F. Vollmer and L. Yang, *Nanophotonics* **2012**, 1, 267-291.
22. F. Vollmer, D. Braun, A. Libchaber, M. Khoshima, I. Teraoka, S. Arnold, *Appl. Phys. Lett.* **2002**, 80, 4057–4059.
23. A. François, M. Himmelhaus, *Sensors* **2009**, 9, 6836-6852.
24. R. Bischler, M. Olszyna, M. Himmelhaus, and L. Dähne, *Eur. Phys. J. Spec. Top*. **2014**, 223, 2041–2055.

25. M. Olszyna, A. Debrassi, C. Üzüm, L. Dähne, *Adv. Funct. Mater.* **2018**, 29(2).
26. S. Pang, R. E. Beckham, and K. E. Meissner, *Appl. Phys. Lett.* **2008**, 92, 2–4.
27. Q. Zhang, Y. Han, W-C. Wang, L. Zhang, J. Chang, *Eur. Polym. J*. **2009**, 45, 2.
28. Multilayer Thin Films– Sequential Assembly of Nanocomposite Materials, (Eds. G. Decher, J. B. Schlenoff), Vol. 1, Wiley VCH, Weinheim, Germany **2012**.
29. J. Kang, L. Dähne, *Langmuir* **2011**, 27, 4627